Aerodynamic and acoustic analysis of helicopter main rotor blade tips in hover

Garipova L.I. [(1)], Batrakov A.S. [(2)], Kusyumov A.N. [(3)], Mikhailov S.A. [(4)], Barakos G. [(5)]

[(1)] Kazan National Research Technical University n.a. A.N.Tupolev, ul. Karla Marksa 10, Kazan, 420111 Tatarstan, Russia, Email: lyaysan_garipova@mail.ru
[(2)] Kazan National Research Technical University n.a. A.N.Tupolev, ul. Karla Marksa 10, Kazan, 420111 Tatarstan, Russia, Email: batrakov_a.c@mail.ru
[(3)] Kazan National Research Technical University n.a. A.N.Tupolev, ul. Karla Marksa 10, Kazan, 420111 Tatarstan, Russia, Email: postbox7@mail.ru
[(4)] Kazan National Research Technical University n.a. A.N.Tupolev, ul. Karla Marksa 10, Kazan, 420111 Tatarstan, Russia, Email: sergey.mikhaylov@kai.ru
[(5)] School of Engineering - The University of Liverpool, Brownlow Hill, Liverpool L693GH, United Kingdom, Email: G.Barakos@liverpool.ac.uk

ABSTRACT

Purpose – The design of main rotor blade tips is of interest to helicopter manufacturers since the tip details affect the aerodynamic performance and acoustics of the rotor. The aim of this paper is the numerical simulation the flow around hovering helicopter blades with different tip designs.

Design/methodology/approach – In this paper, CFD is used to simulate the flow around hovering helicopter blades with different tip designs. For each type of blade tip a parametric study on the shape is also conducted. For comparison, calculations were performed at the same rotor thrust. The collective pitch of the blades and the coning angle of the rotor were determined by an iterative trimming process. The aeroacoustic characteristics of the rotors were obtained using the Ffowcs Williams - Hawkings equation.

Findings – Analysis of the distributed blade loads shows that the tip geometry has a significant influence on aerodynamics and aeroacoustics especially for stations where blade loading is high.

Originality/value – The results are useful for design new blades with high performance and low acoustic emission.

Keywords: CFD, Ffowcs Williams - Hawkings equation, Helicopter, Main rotor, Blade design

Article Type: Research paper

NOMENCLATURE

AR = blade aspect ratio
a = lift slope
a_0 = sound speed
c = chord length
c_n = normalized chord
Cp = pressure coefficient
C_T = thrust coefficient
C_Q = torque coefficient
d = distance from rotor center
f = surface function
I = vortex intensity
M = pitch moment
M_{tip} = tip Mach number
M_r = source Mach number in the direction of noise emission
N = number of blades
p = surface pressure
p' = acoustic pressure
p_0 = ambient pressure of the medium
Δp = perturbation pressure
p_{max} = maximum pressure
p_{min} = minimum pressure
Q = *rotor* torque
q_{tip} = dynamic pressure
R = rotor radius
r/R = normalized rotor radius
r = distance between observer and source
r_P = local blade radius
Re = tip Reynolds number
T = rotor thrust
t = source or emission time
U = blade tip velocity
v_n = local normal velocity of source surface
W_{in} = inflow velocity
W_{out} = *outflow velocity*
x = observer position vector
y = source position vector

Greek symbols
β_0 = coning angle
γ = anhedral angle
η = Lagrangian variable
θ = observer location angle
θ_0 = collective pitch
κ = Lock number
λ= inflow factor
ρ_0 = density of medium
σ = solidity
τ = retarded time
φ = swept angle

Ψ = azimuth angle
ω = angular velocity of rotor, angular frequency of vortex

INTRODUCTION

Research into helicopter blade tips is important for helicopter manufacturers. Past and recent papers demonstrate the constant interest of researchers in this problem. The results show potential to increase the aerodynamic efficiency of the rotor and to reduce its acoustics (aero-acoustic noise). Brocklehurst and Barakos (2012) present a recent review of works dedicated to different aspects of blade tip design. In (Yen, 1994) swept-tapered blade tips were compared with swept, tapered and rectangular versions. In high speed flight the swept-tapered tip reduced the pitch link loads and the blade vibration. Trailing vortex measurements in hover have also been reported in (Martin and Leishman, 2002) for various tip shapes including rectangular, tapered, swept, and a sub-wing tips. One of the primary differences noted was the dependence of wake geometry on the tip shape. The tapered tip reduced the initial swirl velocity, increased the radial convection and decreased the axial convection. The quiet Helicopter demonstrator is discussed in (Allongue et al., 1999). The blade tip shape has a parabolic leading edge and is highly tapered, and therefore has low volume. This tip has some benefits in hover efficiency and noise performance but use on heavier, faster helicopters may be limited by advancing side compressibility effects and retreating side blade stall.

According to (Brocklehurst and Barakos, 2012) three families of blade tips (Figure 1) have so far received attention: parabolic, swept and BERP tips. Further improvements and a reduction of the blade noise can be achieved by modifying the rest of the blade plan form. This was attempted with the “ERATO” (Beaumier and Delrieux, 2003) and “Blue Edge” (Rauch et al., 2011) designs. On the ERATO rotor, the blade curves forward and the main sweep-back starts inboard. The aim of this blade design is to reduce blade-vortex interaction (BVI) noise. Anhedral has been used to on several main rotor designs, and appears to be particularly effective on the BERP-type tip at high rotor loading. In forward flight, anhedral can be useful to balance the effects of sweep and notch offset.

Still, however, there are helicopters with rectangular blade plan forms, mainly due to ease of manufacturing. On the other hand, there is pressure on manufacturers to upgrade and enhance all aspects of their helicopters. The rectangular and swept back planform is also common in helicopters and one of the aims of the present research is to study modifications of this tip shape to improve the aerodynamics and aeroacustics of rotor.

Along these lines, this paper presents research related to the design of a blade for a light multipurpose helicopter similar to the ANSAT helicopter produced by the “Kazan Helicopter Plant”.

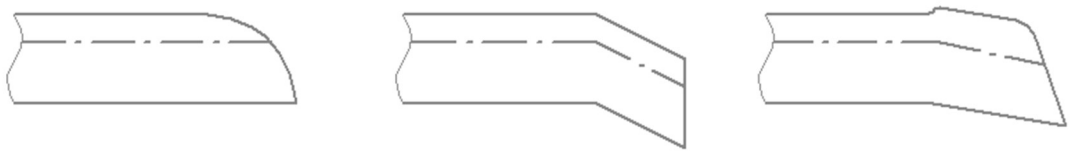

a) b) c)

Figure 1. Popular blade tips: parabolic (a), swept (b) and BERP (c)

1. PROBLEM FORMULATION AND RESEARCH METHOD

This research started by considering the aerodynamic performance of an isolated main rotor helicopter blade in hover. Different tip shapes were compared using Computation Fluid Dynamics (CFD) based on the Reynolds-Averaged Navier-Stokes equations (RANS) closed by k-ω turbulence models. The flow was considered as fully turbulent and compressible. The HMB code (developed at the University of Liverpool, UK) is used (Nik and Barakos, 2012), (Steijl et al., 2006). For hover, a steady-state formulation is employed to reduce the overall computational effort. Structured multi-block grids were constructed around different blade tips using the ICEM-Hexa mesh generation software.

Since temporal and spatial periodicity is assumed for the flow, the computational grid was constructed for a single rotor blade (with appropriate periodic boundary conditions). For the four-bladed rotor at hand, the computational domain is a quarter of a cylinder. The multi-block topology used in this paper, can be seen in Figure 2. Around the blade C-type blocking topology is used. Along the aerofoil surface 340 points are located with concentration near leading and trailing edges. Normal to the surface the first cell size is 10^{-5} of the blade’s chord length and the cell ratio is less than 1.15 following an exponential law.

"Source-sink" boundary conditions (Nik and Barakos, 2010) were obtained from momentum theory and used at all surfaces of the computational domain apart from the symmetry planes. The "periodic" boundary condition provides the periodicity of the flow around the blade. Using the "inflow–outflow" boundary conditions allows for a reduction of the size of the computational domain. The inflow (W_{in}) and outflow (W_{out}) velocities were obtained from momentum theory according to the expressions:

$$W_{in} = -\frac{U}{8}\sqrt{C_T}\left(\frac{R}{d}\right)^2, \quad W_{out} = -U\sqrt{C_T}, \tag{1}$$

where $U = \omega R$ is the speed of the blade tip; C_T is the thrust coefficient; d is the distance from the rotor centre. An initial guess of the rotor thrust coefficient is first used and then the thrust coefficient value is recomputed using successive approximations. The convergence is reached when C_T remains constant (details are given in section 5 of the paper).

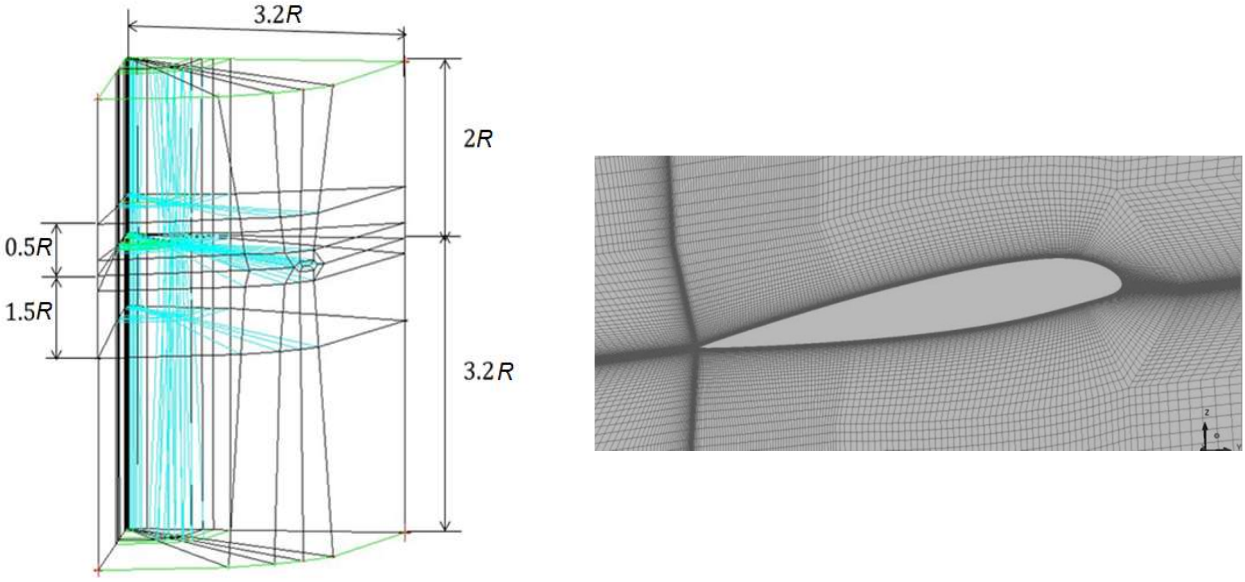

a) b)

Figure 2. (a) Multi-block topology, and (b) mesh section

2. VALIDATION OF CFD RESULTS

The Caradonna-Tung (Caradonna and Tung, 1981) rotor was used for validation of the CFD results in hover since that case is widely used for the validation of CFD codes. The rotor consists of two rectangular, rigidly fixed (on a tall column with a driving shaft) blades, of a NACA0012 airfoil. The blade has the following geometrical parameters: aspect ratio AR = 6, chord length c = 0.1905 m, and rotor diameter $2R$ = 2.286 m.

The selected conditions for computations are shown in Table 1. Simulations were conducted with the k-ω turbulence model. A structured and multi-block computational grid for the Caradonna-Tung rotor consisted of 124 blocks and 5.7 million cells per blade. The distance between the first mesh points above the blade surface was 10^{-5} of the blade's chord length. Given the tip Reynolds number (2.7×10^6), this spacing is necessary for resolving the laminar sub-layer near solid surfaces and for better predictions of the friction drag component. The thrust coefficient (C_T) is determined by the expression:

$$C_T = \frac{T}{q_{tip}\pi R^2}, \tag{2}$$

where q_{tip} is the dynamic pressure at the blade tip and T is the rotor thrust.

Table 1. Conditions for computations of the Caradonna-Tung rotor in hover

Parameters	Values
Collective pitch	θ_0 = 8°
Tip Mach number	M_{tip} =0.612
Tip Reynolds number	Re = 2.7×10^6
Thrust coefficient	C_T = 0.0091
Angular velocity of rotor	ω = 1750 rev/min

The CFD results for the pressure coefficient distribution at different sections of the blade (normalized with the rotor radius, $\bar{r}$) were compared to the experimental data in Figure 3. The comparison shows a good agreement between the numerical results and the experimental data, and is similar to what most researchers have reported (see for example (Tejero et al., 2014), (Doerffer and Szulc, 2008)). A detailed validation of the employed CFD code in terms of integral aerodynamic characteristics of rotors is presented in (Carcia and Barakos, 2016).

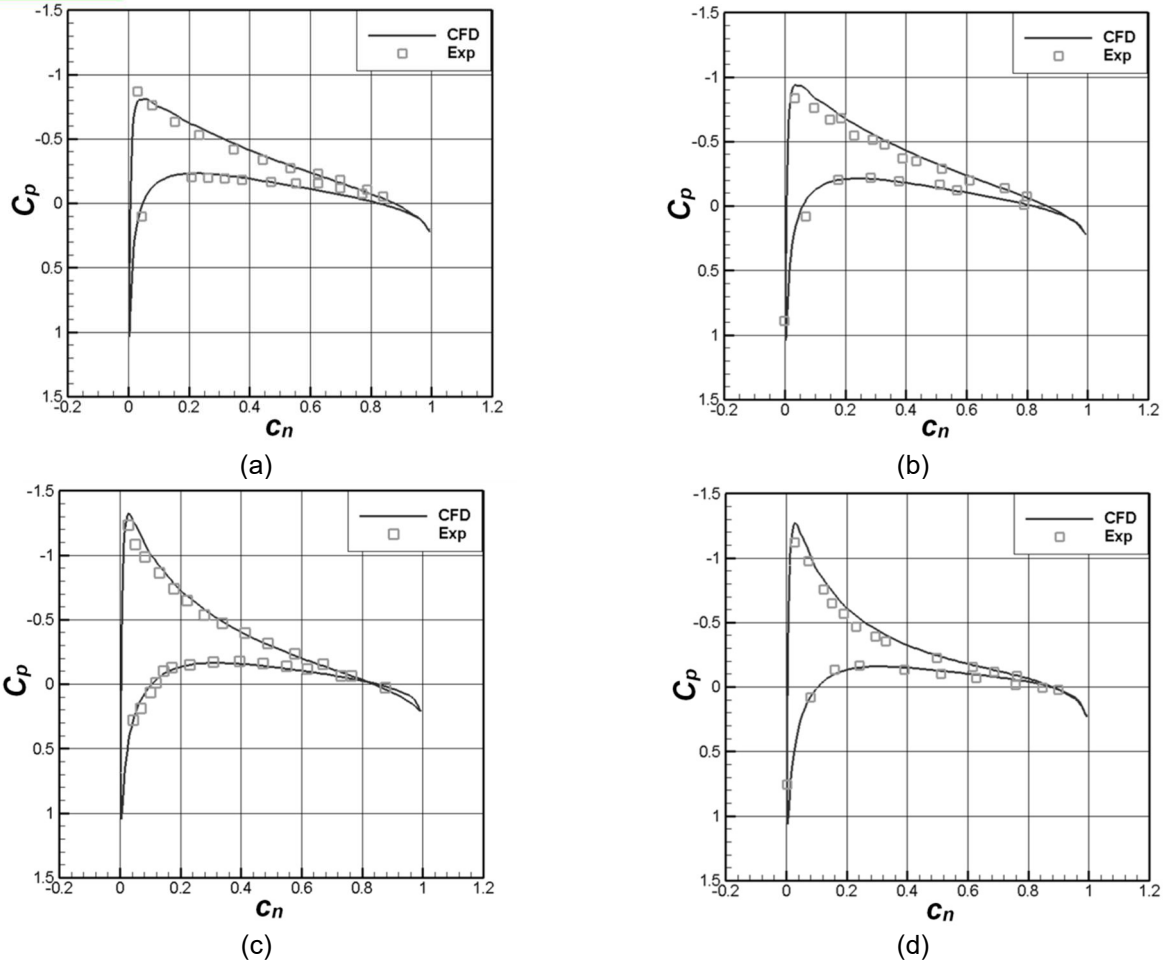

Figure 3. Distribution of pressure coefficient Cp on four Caradonna–Tung rotor sections: (a) *r/R* = 0.5; (b) *r/R* = 0.68; (c) *r/R* = 0.89; (d) *r/R* =0.96.

3. INVESTIGATION OF MESH SENSITIVITY

The light multipurpose helicopter main rotor has four blades. For this new rotor, a similar mesh topology was used like for the Caradonna-Tung case. In addition, a grid sensitivity study was conducted to establish the accuracy of the CFD results. The relatively fine mesh employed here was necessary to achieve well-resolved flows near the blade tip and the mesh quality was kept high up to 0.5*R* (*R* being the radius of rotor) above and up to 1.5*R* below the rotor disk plane (Figure 4). The resulting computational grid had 240 blocks and nearly 28 million cells.

The thrust coefficients obtained on two grids were similar: C_T=0.0102 for the 8.1 million grid and C_T=0.0103 for the 28.2 million grid. However the fine resolves better the blade tip vortices (Figure 4, visualized using *Q* criterion) which are important. On this reason, the fine 28.2 million cells grid was used for comparing rotors with different tips.

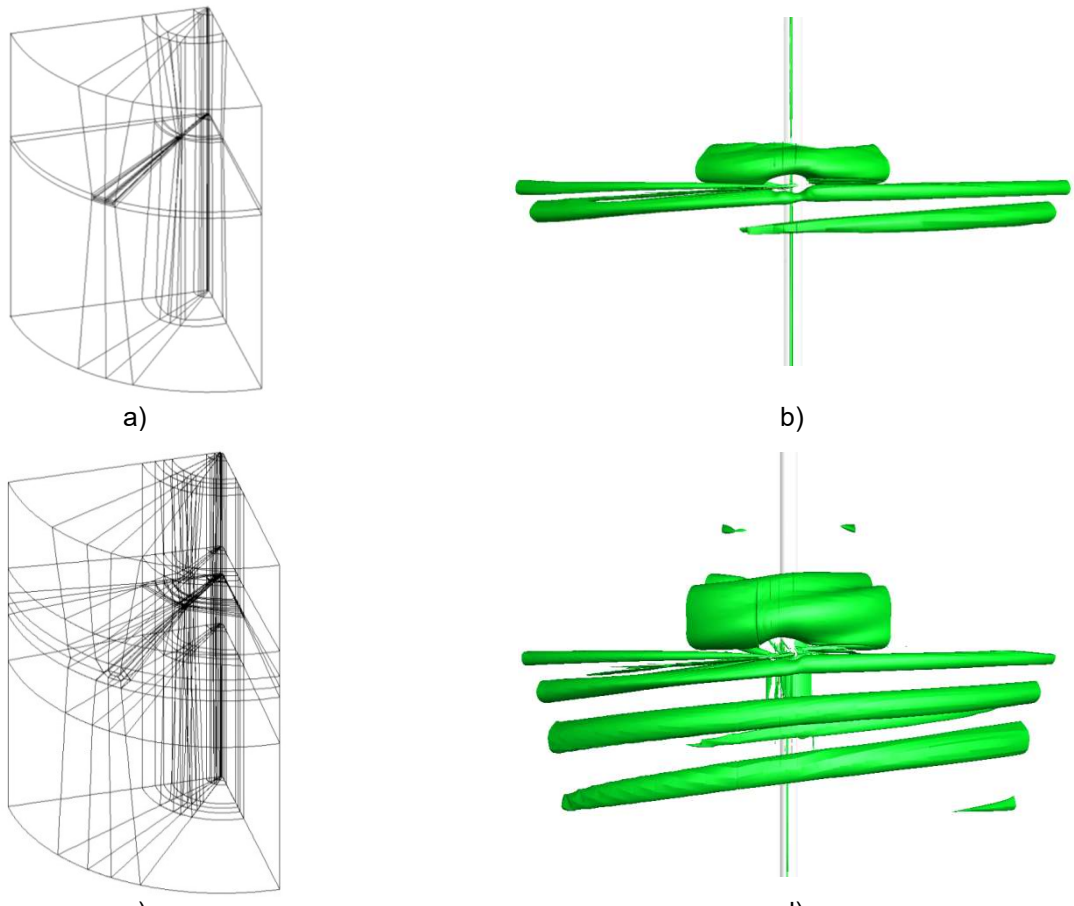

a) b)

c) d)

Figure 4. Grid topology (a), (c) and tip vortex structure according Q-criteria (Q=0.001) (b), (d) for 8.1 million and 28.2 million elements grids, respectively.

4. ROTOR TIP DESIGNS

The baseline main rotor geometry employed for this paper approximates the light multipurpose helicopter main rotor blade. The parameters of the design are presented in Table 2. The baseline design had a rectangular plan form with a simple rounded tip cap (Figure 5.a).

Additional tip designs are shown in Figure 5. It should be noted that the tips used in this work are based on real-world designs: type A (b) approximates the tip of the Mi-8 helicopter, the swept rectangular blade type B (c) is used in Mil, Kamov and other helicopters types. Also the swept (30 degree) rectangular blade with the addition of anhedral, resulting in the Type C tip (Figure 5.d) was considered. For each type of blade tip, different skewness angles were considered and the angle was increased up to 45 degrees (0 degree skewness corresponds to the rectangular blade).

Table 2. Main rotor parameters

Rotor geometry	
Number of blades, N	4
Diameter of the rotor, $2R$ (m)	11.5
Twist of blade, degrees	-5.3
Root cut-out, %R	0.20
Reference blade chord, c (mm)	320
Thickness of the blade section, %c	12
Conditions for computations	
Collective pitch angle, degrees	θ_0 = 8
Tip Mach number	M_{tip} =0.64
Tip Reynolds number, millions	Re = 4.7

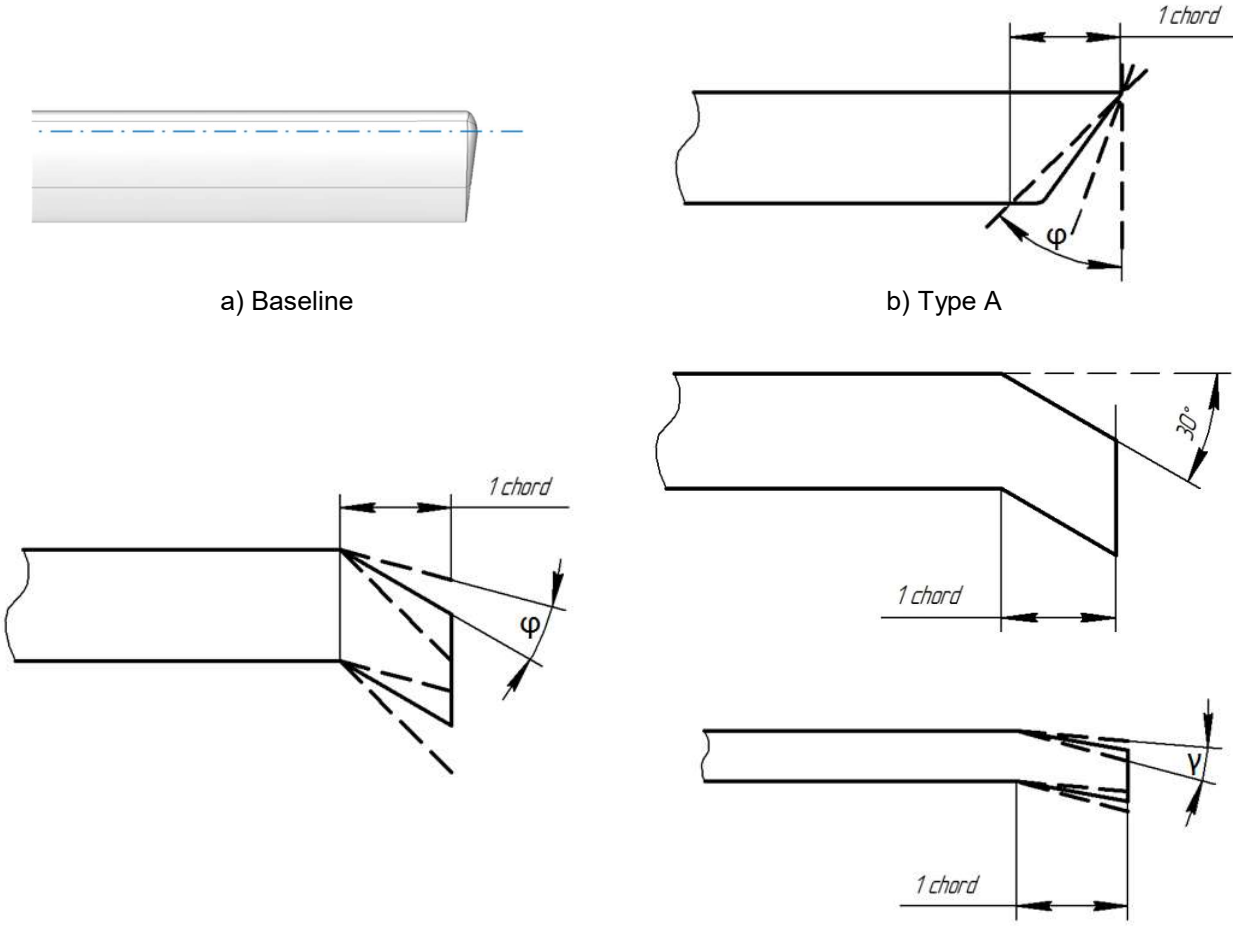

a) Baseline b) Type A

c) Type B d) Type C

Figure 5. Main rotor blade tip designs: a) Baseline; b) Type A; c) Type B; d) Type C

5. BLADE TRIMMING CONDITIONS

A comparative analysis of the rotor performance with different blade tips geometry requires comparisons at the same thrust C_T coefficient. This requires trimming of the rotor blade by changing the collective θ_0 and coning β_0 angles. The trimming procedure algorithm is presented in Figure 6.

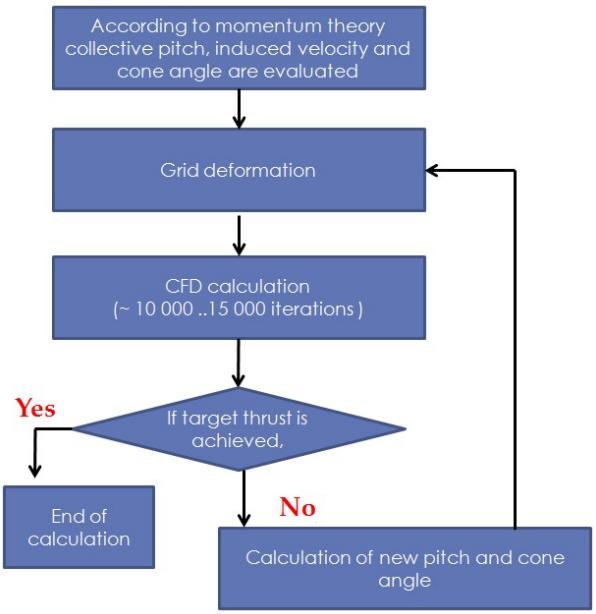

Figure 6. The trimming algorithm

The mathematical formulation of the trimming procedure consists of the following steps.

1. At start-up, an initial estimate of the trim state is computed using the following equation for the collective pitch:

$$\theta_0 = \frac{6}{\sigma a} C_T + \frac{3}{2}\sqrt{\frac{C_T}{2}}. \tag{3}$$

Here, σ is solidity, and *a* is lift slope of aerofoil. In this case, the inflow factor λ can be obtained directly from the equation:

$$\lambda = -\sqrt{\frac{C_T}{2}} = -\frac{\sigma a}{16}\left[\sqrt{1+\frac{64}{3\sigma a}\theta_0} - 1\right]. \tag{4}$$

assuming a constant inflow in the rotor disk. For a twisted rotor blade, equation (3) gives the collective pitch at 0.75 of the rotor radius *R*. Then, the conning angle β_0 is:

$$\beta_0 = \frac{\kappa}{8}\left[\theta_0 + \frac{4}{3}\lambda\right]. \tag{5}$$

2. The mesh is then deformed to account for the new rotor blade incidence and position.
3. A steady flow simulation is performed until a prescribed level of convergence is reached.
4. After few steps, a re-trimming is performed. The collective is updated using the following relation:

$$\delta\theta_0 = \frac{C_{T,\mathrm{target}} - C_T}{\frac{dC_T}{d\theta_0}}, \quad \frac{dC_T}{d\theta_0} = \frac{\sigma a}{6}\left[1 - \frac{1}{\sqrt{1+\frac{64}{3\sigma a}\theta_0}}\right]. \tag{6}$$

Equation (5) gives the conning angle for the new collective pitch $\theta_0+\delta\theta_0$.

5. Steps 2-4 are repeated until a constant trim state is reached.

The typically history of the trimming process for rotor in hover is presented in Figure 7 (the trimming process is presented for blade type C). It is shown that 70000 iterations are enough to meet the target thrust (grey solid line). Results of trimming process were considered satisfactory if the thrust coefficient is in the range 0.01±0.0005.

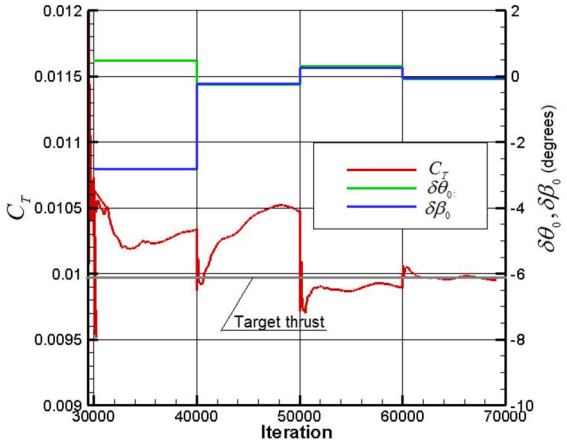

Figure 7. Typical history of the trimming process

6. PERFORMANCE ANALYSIS

A comparative analysis of the aerodynamic characteristics of the rotor blade tips was conducted with the thrust corresponding to the max take-off weight of a light helicopter.

The torque (C_Q) and the figure of merit coefficients are determined as

$$C_Q = \frac{Q}{q_{tip}\pi R^3}, \; FoM = \frac{C_T^{1.5}}{2C_Q}, \tag{7}$$

Where *Q* is the rotor torque.

The comparisons of modelling results for the trimming are presented in Figure 8. In this figure the normalized values for the C_Q and *FoM* are shown. Normalization was conducted according to the expressions:

$$C_{Qn}(\varphi)=C_Q(\varphi)/C_Q(0), \qquad FoM_n(\varphi)=FoM(\varphi)/FoM(0). \tag{8}$$

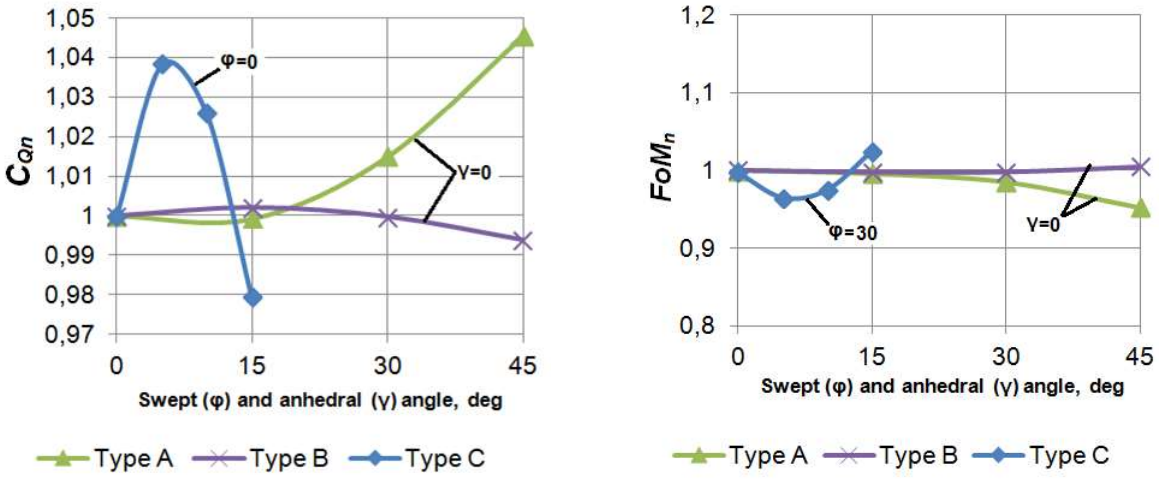

Figure 8.Comparison of normalized integral performances

Analysis of the integral characteristics shows that changes of the blade tip can lead to improve of the integral characteristics relative to the baseline configuration. However, it can be noted that modifications like type A lead to increased torque and lower figure of merit. From the given research it follows also that the dependence of *FoM* on anhedral angle has non-monotonic character with decreasing of the *FoM* values for the small anhedral angles.

The analysis of the spanwise integrated blade loads (Figure 9) shows that modifications like type A lead to increased torque at tip part of the blade. Modifications like type B and type C lead to decreasing torque and to significant increasing of pitch moment at the tip part of the blade. Another problem is that shape with the extreme swept-back tip will leads to an increasing of the blade control loads in forward flight. Modifications like type C lead to decreasing thrust at the tip part of the blade and this may be reason for decreased load noise.

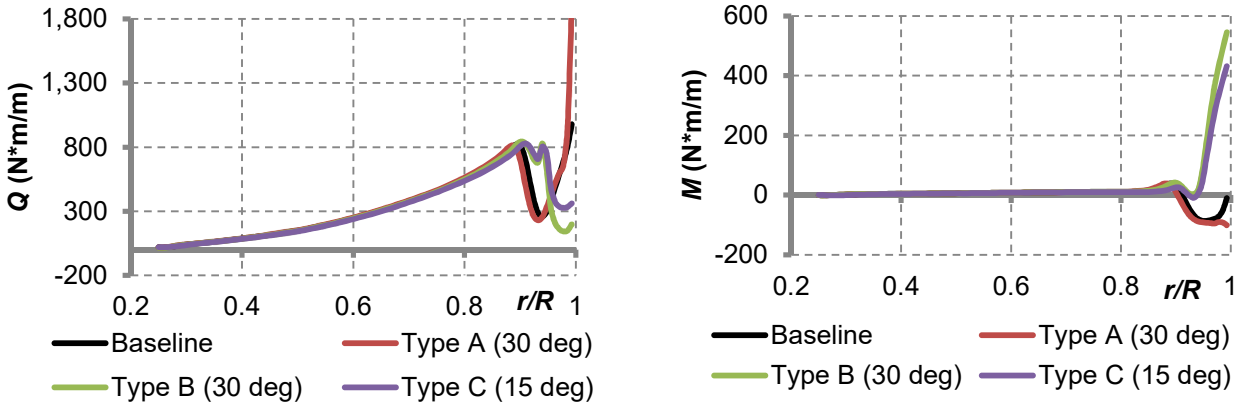

a) b)

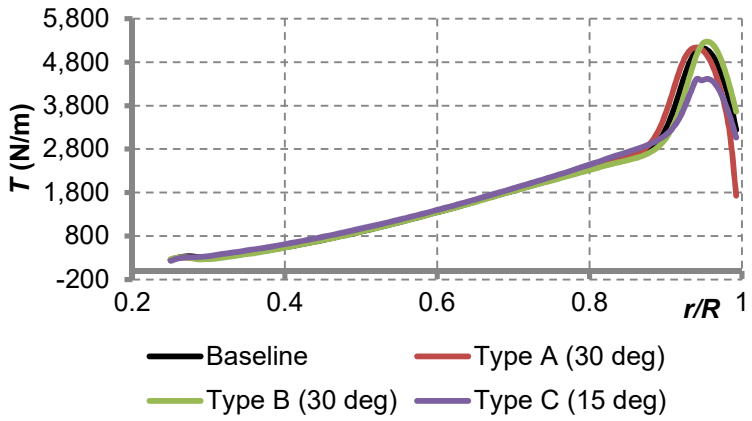

c)

Figure 9. Blade spanwise load distributions: a) torque distribution; b) pitch moment distribution; c) thrust distribution

7. FFOWCS WILLIAMS – HAWKINGS EQUATIONS

Aerodynamic coefficients are important, but are only one of the indicators of blade efficiency. Nowadays the aeroacoustic properties of the rotor blades are also accounted for during blade design. Aeroacoustic modelling in general requires the use of URANS equations and advanced turbulence models, for proper predictions of the Sound Pressure Level (SPL) and spectral analysis of sound generation. The steady formulation of the CFD method does not allow a detailed analysis of blade acoustics.

The helicopter main rotor generates tonal and broadband noise. The tonal noise, in general, is usually divided into the deterministic components of thickness and loading noise, BVI noise and high-speed impulsive (HSI) noise (Brentner and Farassat, 2003). Similarly, broadband noise consists of the non-deterministic loading noise sources classified as turbulence ingestion noise, blade-wake interaction noise and blade self-noise.

A widely used method for predicting the aerodynamically generated rotor noise is based on the Ffowcs Williams – Hawkings (FW–H) equation (Ffowcs Williams and Hawkings, 1969). Implementation of the FW–H equation to CFD methods is usually based on the integral formulation of the FW–H equation. The general FW-H equation formulation includes several terms, including the sickness, load and quadrupole terms. For the relatively Mach number value and hover mode the quadrupole term (corresponding to the HIS noise) is neglected according to paper (Brentner and Farassat, 2003).

The far field retarded-time formulation by Farassat is commonly referred to as Formulation 1 (Brentner and Farassat, 2003):

$$4\pi p`(\mathbf{x},t) = \frac{1}{a_0}\frac{\partial}{\partial t}\int_{f=0}\left[\frac{\rho_0 a_0 v_n + l_r}{r\left|1-M_r\right|}\right]_{ret} dS. \tag{9}$$

Here a_0 is sound speed; $f = 0$ is a function that describes the source surface; ρ_0 is the density of medium; v_n is the local normal velocity of source surface; M_r is the source Mach number in radiation direction; r is the distance between observer and source, $r = |\mathbf{x} - \mathbf{y}|$, $\mathbf{x}$ is the observer position vector, with components x_i, $\mathbf{y}$ is the source position vector, with components y_i; $p' = p - p_0$ is the acoustic pressure, p_0 is the pressure of the medium, p is the surface pressure; l_r are the components of the local aerodynamic force intensity. The subscript ret denotes the retarded time and the integration is performed over the actual blade surface $f = 0$. For a moving surface the retarded time τ is determined by the expression

$$\left|\mathbf{x} - \mathbf{y}(\eta,\tau)\right| = a_0(t-\tau),$$

where t is the source or emission time, and η is the Lagrangian variable of a point on the moving surface.

Equation (9) can be rewritten in the form (Ffowcs Williams and Hawkings, 1969):

$$p`(\mathbf{x},t) = p`_T(\mathbf{x},t) + p`_L(\mathbf{x},t). \tag{10}$$

Here

$$p`_T(\mathbf{x},t) = \frac{1}{4\pi}\frac{\partial}{\partial t}\int f=0\left[\frac{\rho_0 v_n}{r\left|1-M_r\right|}\right]_{ret} dS \tag{11}$$

is the thickness noise, and

$$p`_L(\mathbf{x},t) = \frac{1}{4\pi a_0}\frac{\partial}{\partial t}\int_{f=0}\left[\frac{l_r}{r\left|1-M_r\right|}\right]_{ret} dS \tag{12}$$

is the load noise.

For a hovering rotor of radius R the singularity point, emitting a disturbance at position "P" with local blade radius r_P ($r_P < R$), travels at the ambient speed of sound and arrives at the observer's position "0" with the time delay r/a_0.

According to the formulas (10)-(12), to determine the total rotor noise at the observer location point it is necessary to know the geometry of blade and the rotor disk pressure distribution. For some cases of the observer location contribution of the noise components can be significantly different. So, dominant source of noise for in-plane is the thickness noise. There are very few publications presenting experimental data used for validation of algorithms and programs based on the FW–H equation. Widely used experimental data can be found in paper (Shmitz and Yu, 1986). That paper presents flight tests data and hover wind tunnel data for high Mach number values (M=0.8 and higher). Paper (Carcia and Barakos, 2016) presents a comparison of the FW–H solution with theory.

In the present research, we follow the approach adopted in (Arda et al., 2014) that presents experimental data of acoustic measurements of the main rotor of a light weight helicopter in hover mode for moderate values of Mach number. In (Arda et al., 2014) tests were conducted on the whirl tower at hover conditions for different microphone locations, including in-plane position. The specifications of the tested prototype are presented in Table 3.

Table 3. Rotor parameters

Blade span	3 m
Chord	0.173 m
Nominal rotational speed	540 rpm
Twist Angle	16˚
Cone angle	2˚
Root-Cut Out	10%

Reference (Arda et al., 2014) does not provide the full geometry of the blade. Nevertheless the data of the paper (Arda et al., 2014) can be used for a qualitative comparison of the rotor noise modelling results to the experiment data. Figure 10 presents experimental data for the rotor thickness noise SPL from the paper (Arda et al., 2014) compared to the FW-H (11) solution (thickness noise only) for different rotational frequencies. The small discrepancy between the theory and experiment data for the low RPM values can be explained by the lack of the detailed rotor geometry used for experiments. For simulations, the NACA 0012 aerofoil was used for the FW-H equation. Possible influences of other noise sources are broadband noise, for example were neglected.

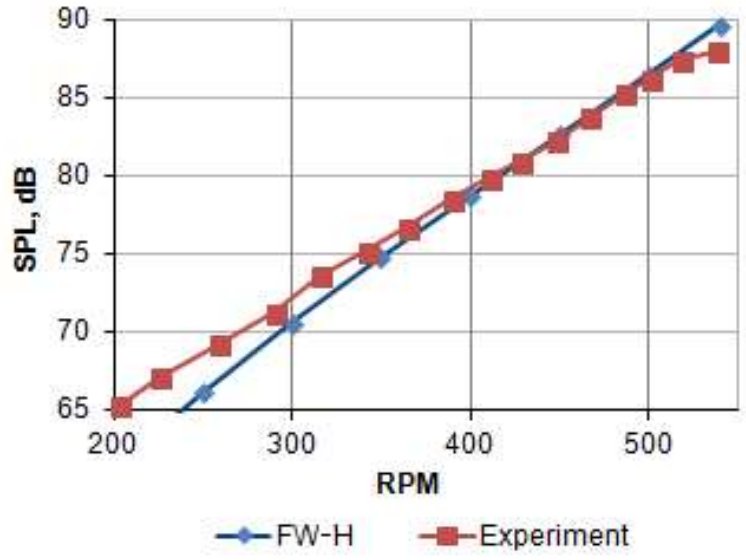

Figure 10. Comparison between calculations and experiments for the noise of a light weight helicopter

The FW-H approach was also used for comparisons of the acoustic SPL, for different blades: baseline, types A, B and C (Figure 5). Figure 11 presents the total noise diagram for observers located according Figure 11.a. These observers are located at a distance of 3*R* from rotor; the blade tip Mach number was 0.64. In the plane of rotor rotation, the thickness noise is the main contribution to the total noise. The loading noise contribution is more pronounced away of the rotation plane and leads to higher SLP.

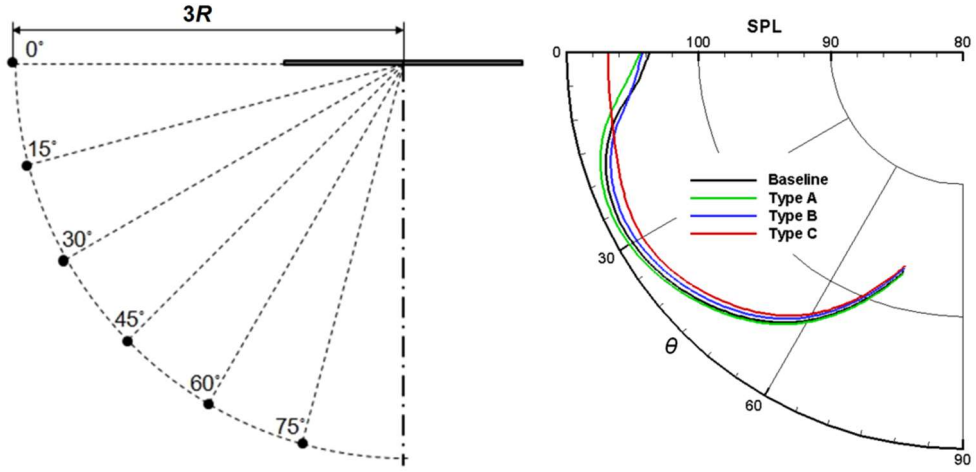

a) b)

Figure 11. Acoustic diagram: a) location of observers; b) total noise diagram (SPL, dB)

From Figure 11.b, it can be concluded that the anhedral tip decreases the peak sound pressure level for the higher observation angles.

Proceeding from Figure 11 one can conclude that the blade tip aeroacoustics varies with the observer location: for an inplane observer the maximum SPL corresponds to the type C blade tip; on the contrary for the out-of-plane observer blade C is quieter (because of the reduction of the loading noise).

8. VORTEX INTENSITY ANALYSIS AND ACOUSTIC PROPERTIES OF THE BLADE TIPS

In the present paper we compare the aeroacoustic properties of blade tips near the rotor. The study of the rotor aeroacoustic is based on the FW-H equation. This approach presents information about the SPL level, but it does not allow estimation of aeroacoustic properties of the near field of the rotor blades. In the present item, we consider some additional properties of flow, including the tip vortex intensity and the near field pressure perturbation in the area of blade tip using the results of numerical modelling.

The tip vortex intensity presents the integral estimation of the vortex core angular frequency, as determined by basic vortex structures generated in the blade passing process. The tip vortex in itself has been the subject of several publications, including experimental (Martin and Leishman, 2002) and numerical studies (Kang and Kwon, 2001).

Figure 12a presents the structure of tip vortex for the baseline blade visualized using Q criterion at different vortex sections and Figure 12b shows comparison of the vortex core location to the Kocurek - Tangler theory (Kocurek and Tangler, 1977). The intensity of the tip vortex is determined by perturbations of flow generated by the blade surface. Hence the blade tip vortex intensity value can be considered as objective parameter of the blade acoustics.

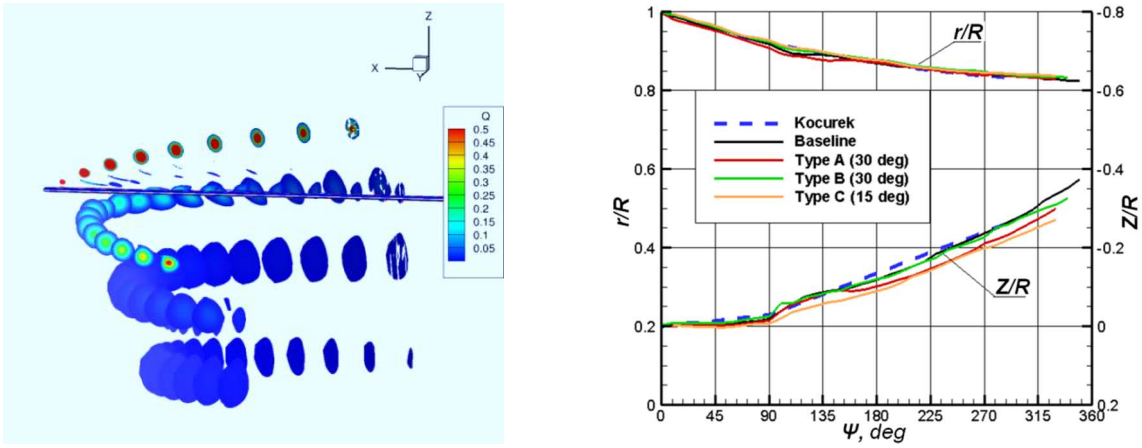

a) b)

Figure 12. Blade tip vortex (a); radial R and axial Z coordinates of the tip vortex, normalized to the rotor radius (b)

Comparison of the vortex core properties can be performed using the intensity of the vortex core computation. The intensity of the vortex core is determined by the integral:

$$I = \iint \omega dS, \tag{13}$$

where ω is the angular frequency, S is cross-sectional area of the vortex core (the area of vortex core is limited by a minimal value of the angular frequency of 20Hz).

The variation of the blade tip geometry leads to a redistribution of the load and is expected that the vortex position will also change. Analysis of the tip vortex intensity was considered for a radial section located at 30 degrees of azimuth angle (relatively to the blade trailing edge). Distributions of the angular velocity of the tip vortex at the control section are presented for different types of plane form in Figure 13. The figures show that the blade tip shape affects both the tip vortex intensity, and spatial vortex position.

The maximum values of the tip vortex angular frequency (at the considered section) and the vortex core intensity are presented in Figure 14a and 14b.

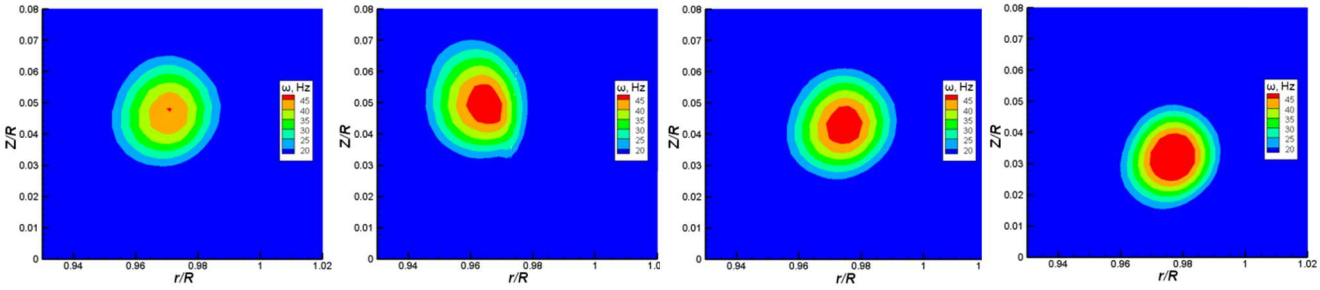

a) b) c) d)

Figure 13. Distribution of the angular frequency of the blade tip vortex:
a) baseline; b) type A (30°); c) type B (30°); d) type C (15°)

From the analysis of the simulation results, it follows that considered modifications lead to increase tip vortex intensity.

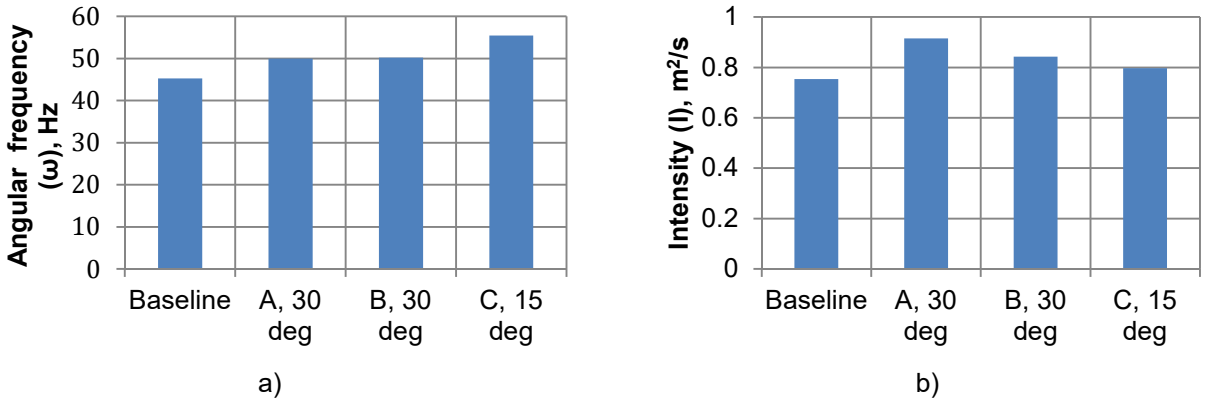

a) b)

Figure14.Tip vortex intensity parameter: a) peak values of the angular frequency ω; b) vortex intensity I (m^2/s)

The near field pressure perturbation analysis was conducted for an array of 9 microphones located vertically at a distance the 30 cm from the tip part of the blade. Figure 15 presents local microphone pressure perturbations $\Delta p=p_{max}-p_{min}$ values for the considered blade tips (p_{max} and p_{min} are maximum and minimum microphone pressure values per one rotor revolution).

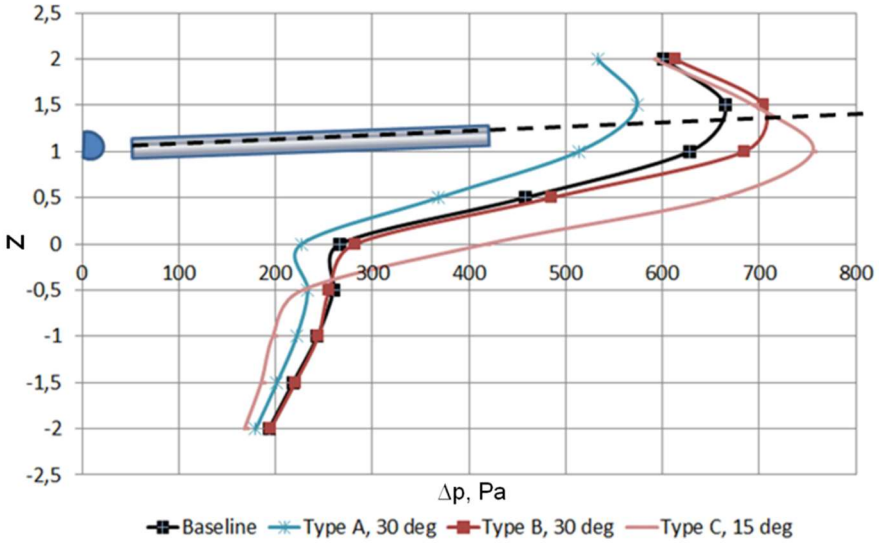

Figure 15. Local pressure perturbation values for the set of blades

Figure 15 shows some discrepancy between locations of the maximum values of the local SPL level: for the baseline blade, blades of A, B types on the one hand and the blade of C type. For the first three tips the maximum of the SPL level is located close to a line, extending outwards, along the axis of the blade (dashed line in Figure 15.); for blade C the maximum of SPL is located below dash line (it is evidently because of anhedral of the blade).

Comparing Figures 14, 15 and 11 one can conclude that there is some correlation between the vortex angular frequency and local SPL level. Maximum values of SPL and maximum values of the vortex angular frequency can be seen for blade C close to the rotor disc

Comparison of results (Figure 15) for different blade tip types shows, that type A leads to less pressure perturbations. It can be concluded that the blade tip type A provides less sound generation. There is opposite situation for types B and C. We can note also some contradiction between aerodynamic and aeroacoustic properties requirements for the trimmed rotor: the minimal sound generation corresponds to the blade with a lower *FoM*.

9. SUMMARY AND FUTURE WORK

This paper presents a study on the influence of blade tip parameters to hover performance. The analysis of the rotor tips showed that the tip shape influences both aerodynamics and acoustics and gains

can be made on both fronts if the tip-design is conducted with care. The baseline main rotor geometry employed for this paper, with the rectangular plan form, and the simple rounded tip cap approximates the light multipurpose helicopter main rotor blade. Additional tip designs used in this work are based on real-world designs: type A approximates the tip of the Mi-8 helicopter, the swept rectangular blade type B is used in Mil, Kamov and other helicopters types. Also the swept (30 degree) rectangular blade with the addition of an anhedral angle(15 degrees) was considered.

In comparison to the baseline (rectangular plane form) blade, better aerodynamic performance was demonstrated by the type C blade. It was demonstrated also that the dependence of FoM on anhedral angle has non-monotonic character with decreasing of the FoM values for the small anhedral angles.

The blade aeroacoustic efficiency varies with the observer location: for inplane observer maximum of SPL corresponds to the type C blade (inplane observer) tip; on the contrary for the outplane observer, blade C reveals better aeroacoustic performance.

One can conclude that there is some correlation between the vortex angular frequency and local SPL level for the near field observer. Maximum values of SPL and maximum values of the vortex angular frequency were seen for blade C close to the rotor disc

Once the hover mode was investigated, further computations will evaluate the rotor performances in forward fight.

ACKNOWLEDGEMENTS

This work was supported by the “State tasks in the field of scientific activity” (No 9.1694.2014/K) Grant.

REFERENCES

Allongue, M., Marze, H.J. and Potdevin, F., (1999), “The Quiet Helicopter - From Research to Reality”, In *55th Annual Forum of the American Helicopter Society, Montreal, Canada*, May 1999.

Arda Yücekayali, Erdem Ayan, Yüksel Ortakaya, (2014), “Acoustic assesment of 3 meter radius rotor with whirl tower test and analysis”, *AHS 70th Annual Forum*, Montréal, Québec, Canada, May 20–22, 2014. p. 1-9. AHS2014-000278.pdf.

Beaumier, P. and Delrieux, Y. (2003), “Description and Validation of the ONERA Computational Method for the Prediction of Blade-Vortex Interaction Noise”, in *29th European Rotorcraft Forum*, Friedrichshafen, Germany, September 2003, 1-15 pp., p010.pdf.

Brentner, K. S., Farassat, F. (2003), “Modeling Aerodynamically Generated Sound of Helicopter Rotors”, *Progress in Aerospace Sciences*, 39, pp. 83-120.

Brocklehurst, A. and Barakos, G.N. (September, 2012), “A Review of Helicopter Rotor Blade Tip Shapes”, *Progress in Aerospace Sciences*, 1-36 pp. (http://dx.doi.org/10/1016/j.paerosci.2012.06.003).

Caradonna F. X. and Tung C. (1981), “Experimental and analytical studies of a model helicopter rotor in hover”, NASA TM-81232, 1981, 58p.

Carcia A.J. and Barakos G.N., (2016), “Hover Predictions of the S-76 Rotor using HMB2-Model to Full-Scale”, in *54th AIAA Aerospace Sciences Meeting*, 4-8 January 2016, San Diego, California, USA.

Doerffer P., Szulc O. (2008), “Numerical simulation of model helicopter rotor in hover”, in *Task Quarterly,* Volume 12, No 3, pp. 227-236.

Ffowcs Williams, J. E., Hawkings, D. L. (1969), “Sound Generation by Turbulence and Surfaces in Arbitrary Motion”, *Philosophical Transactions of the Royal Society*, Volume 264, issue 1151, (08 May 1969) 321-342 pp.; DOI: 10.1098/rsta.1969.0031.

Kang, H.J., Kwon, O.J., (2001), “Viscous Flow Simulation of a Lifting Rotor in Hover Using Unstructured Adaptive Meshes”, *AHS 57th Annual Forum,* Washington, DC, May 9-11, 2001. p.1-13.

Kocurek, J.D. and Tangler, J.L. (1977), “A Prescribed Wake Lifting Surface Hover Performance Analysis”, *J. of the American Helicopter Society*, 1977, vol. 22, no. 1, pp. 24–35

Martin, P.B. and Leishman, J.G. (2002), “Trailing Vortex Measurements in the Wake of a Hovering Rotor Blade with Various Tip Shapes”, in *58th Annual Forum of the American Helicopter Society, Montreal, Quebec,Canada*, June 2002.

Nik A. Ridhwan Nik Mohd and Barakos, G.N., (2012), “Computational Aerodynamics of Hovering Helicopter Rotors”, *Jurnal Mekanikal*, 2012, no. 34, pp. 16–46.

Nik A. Ridhwan Nik Mohd and Barakos, G. N. (2010), “Computational Aerodynamics of Hovering Helicopter Rotors”, *RAeS Aerodynamics Conference*, July 27–28, 2010, University of Bristol, UK.

Rauch, P., Gervais, M., Cranga, P., Baud, A., Hirsch, J-F., Walter, A., Beaumier, P. (2011), “Blue Edge™: The Design, Development And Testing Of A New Blade Concept”, in *AHS-67 conference,* Virginia Beach, VA, May 3-5, 2011, p. 1-14, AHS2011-000043.pdf.

Shmitz F.H. and Yu Y.H. (1986), “Helicopter impulsive noise: theoretical and experimental status”, *Journal of Sound and Vibration,* Vol. 109, No. 3, 1986, pp. 361-422.

Steijl, R., Barakos, G., and Badcock, K. (2006), “A Framework for CFD Analysis of Helicopter Rotors in Hover and Forward Flight”, in *Journal for Numerical Methods in Fluids*, 2006, vol. 51, no. 8, pp. 819–847.

Tejero F., Doerffer P., Szulc O. (2014), “Aplication of passive flow control device on helicopter rotor blades”, in *40-th European Rotorcraft Forum,* Southampton, UK, September 2-5, 2014.

Yen, J.G. (1994), “Effects of Blade Tip Shape on Dynamics, Cost, Weight, Aerodynamic Performance, and Aeroelastic Response”, *Journal of the American Helicopter Society*, 39(4):37–45, October 1994.